

This is a reprint of a paper intended for publication in a journal or proceedings. Since changes may be made before publication, this reprint is made available with the understanding that it will not be cited or reproduced without the permission of the author.

UCRL - 77080 Rev 1  
PREPRINT

CONF-75/130-30

MASTER



LAWRENCE LIVERMORE LABORATORY  
University of California/Livermore, California

NOTICE  
This report was prepared as an account of work sponsored by the United States Government. Neither the United States nor the United States Energy Research and Development Administration, not any of their employees, nor any of their contractors, subcontractors, or their employees, make any warranty, express or implied, or assume any legal liability or responsibility for the accuracy, completeness or usefulness of any information, apparatus, product or process disclosed, or represents that its use would not infringe privately owned rights.

LASER IRRADIATION OF THIN PLASTIC TARGETS  
WITH A 10.6  $\mu\text{m}$  CO<sub>2</sub> LASER

K. R. Manes, R. A. Haas, V. C. Rupert, M. J. Boyle

December 1975

This Paper was Prepared for Submission to  
the APS Meeting, St. Petersburg, Florida,  
November 10-14, 1975

OT W-7405-ENG-48

80

## LASER IRRADIATION OF THIN PLASTIC TARGETS

### WITH A 10.6 $\mu\text{m}$ $\text{CO}_2$ LASER

Work performed under the auspices  
of the U.S. Energy Research &  
Development Administration under  
contract No. W-7405-Eng-48.

#### Vugraph 1

Polyethylene foils and parylene disks 5 to 10  $\mu\text{m}$  thick have been irradiated by  $\text{CO}_2$  laser pulses focused to flux levels in the  $10^{13}$  to  $10^{14}$   $\text{W}/\text{cm}^2$  range. In this talk I will describe our facility and compare the results obtained on these experiments to similar targets hit with 1.06  $\mu$  pulses of like intensity. A  $\text{CO}_2$  laser system, "Valkyrie," fabricated from commercially available components was assembled for these experiments. In the background the actively mode-locked oscillator and preamplifiers which use Lumonics TEA discharge gain media may be seen. The switched-out nanosecond pulse is next amplified by two cold-cathode electron-beam sustained amplifiers built by Systems, Science, and Software, Inc. After passing through the beam diagnostics tables, the beam is finally focused on the target in the chamber in the foreground.

#### Vugraph 2

Schematically Valkyrie looks like this. Its unique features are its two stage electro-optic switch-out system, high beam quality afforded by large aperture uniform gain amplifiers, and low electrical noise due to careful shielding. Reliable 10 to 30 J pulses with durations of 1.5 to 3 ns with no detectable parasitic oscillations, and prepulses  $< 33$  db down were provided for target experiments.

#### Vugraph 3

The 10.6  $\mu\text{m}$  laser beam diagnostics are shown on this slide. Besides incident energy we monitored forward scattered, backscattered and side-scattered light; pulse duration; prepulse extinction ratio, near field energy distribution and focal spot energy distribution.

#### Vugraph 4

These data are presented to demonstrate the quality of the 10.6  $\mu\text{m}$  laser beam. The left trace shows the results of the prepulse extinction measurement which reveals the degradation of the extinction ratio caused by saturation of the selected pulse during amplification. On the right are shown the near field and focal energy distributions. In both cases the profiles are nearly Gaussian.

#### Vugraph 5

The targets placed in this beam are shown here. Both types of targets were located within 100  $\mu\text{m}$  of the true focus well within the  $\sim 1.4$  mm Rayleigh range of the focused beam. The beam is thus collimated at the target.

#### Vugraph 6

Mounted in the vacuum chamber the target is viewed by an array of plasma diagnostic devices.

#### Vugraph 7

The target diagnostics configuration is shown in this slide. Detailed measurements of the ion, electron (30 keV-180 keV), and x-ray emission spectra were made on each shot. Streak photographs of the blowoff plasma and accelerated foil were made with an S-20 ultrafast streak camera. A slower STL camera insured that any preheat due to a prepulse would be seen.

#### Vugraph 8

One of the most striking experimental results obtained was evidence of localized plasma heating which could be due to trapping and/or filamentation

of the laser beam. For comparison, on the left is shown the density contours of an x-ray pinhole photograph of a 1.06  $\mu\text{m}$  laser produced plasma. Although the laser beam had several hot spots, there is a notable absence of any detailed features and the intensity declines monotonically from a central maximum. By contrast, the right side of this slide shows detailed structures smaller than the diffraction limit of the 10.6  $\mu\text{m}$  laser beam. This is evidence of localized heating.

#### Yugraph 9

The results presented on the previous slide are consistent with theoretical prediction of laser beam filamentation by Kow, Scmidt and Wilcox. Shown here are the calculated self focus length and filament width for 1.06  $\mu$  and 10.6  $\mu$  laser experiments. Filamentation is predicted for the 10.6  $\mu\text{m}$  laser beam but not for the 1.06  $\mu\text{m}$  laser beam. The filament width  $\sim$  40 to 60  $\mu\text{m}$  is in agreement with the dimensions of the spots observed in the 10.6  $\mu\text{m}$  irradiations. Calculations assuming a Gaussian beam geometry as well as detailed numerical simulations reveal much the same behavior.

The following four slides will present additional comparisons between 10.6  $\mu\text{m}$  and 1.06  $\mu\text{m}$  irradiations of comparable energy and pulse duration.

#### Yugraph 10

10.6  $\mu\text{m}$  experiments with  $I_p$  in the  $10^{13}$  to  $10^{14}$   $\text{W}/\text{cm}^2$  range have generally shown lower x-ray conversion efficiency and a strong angular dependence. This implies that the bulk of the 10.6  $\mu\text{m}$  heated plasma has simply not reached temperatures typical of comparable 1.06  $\mu$  shots.

Vugraph 11

Substantial light refraction around instability dominated plasmas in the 10.6  $\mu$  case is suggested by the charged particle spectra observed. This slide compares electron emission spectra taken at 45° on 1.06  $\mu$ m and 10.6  $\mu$ m experiments. The loss of such a large number of electrons would raise the target to megavolt potentials were it not for conduction paths to the target mounting structures. Variations in spectra correlate with differences in target geometry as demonstrated here.

Vugraph 12

Ion emission energy distributions also demonstrate a target geometry dependence in 10.6  $\mu$ m experiments not observed in 1.06  $\mu$ m studies. This slide compares large area foils to finite size disks. Easily refracted 10.6  $\mu$ m light impinges upon and heats the foils over a large area producing a large quantity of low energy ions.

Vugraph 13

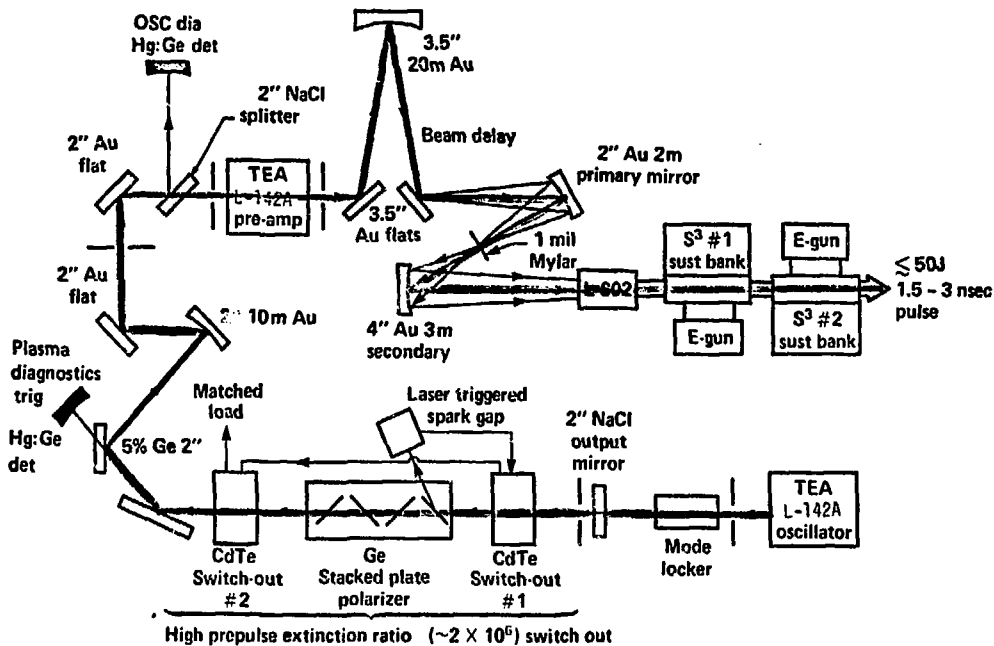
Finally, streak photographs reveal relatively low velocities imparted to the luminous plasmas on the back surface of 10.6  $\mu$ m irradiated targets. Substantially larger foil accelerations for comparable experimental conditions have been observed in 1.06  $\mu$ m events.

Summary:

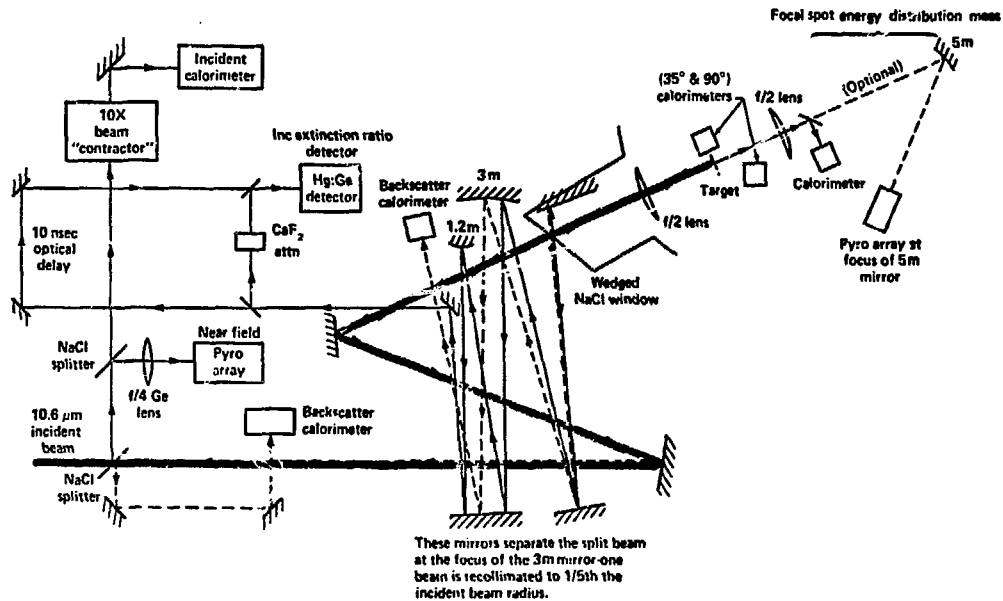
1. We see localized heating in 10.6  $\mu$  but not 1.06  $\mu$  heated plasma
2. 10.6  $\mu$  plasmas exhibit lower x-ray conversion - more refraction  
(don't have number - looked like ~ all was refracted!)
3. Heating pellets to produce spherical implosions by electron  
conduction. Using 10.6  $\mu$  is doubtful.



# VALKYRIE CO<sub>2</sub> LASER SYSTEM



# VALKYRIE LASER BEAM DIAGNOSTICS



## VALKYRIE CO<sub>2</sub> INCIDENT LASER BEAM CHARACTERISTICS

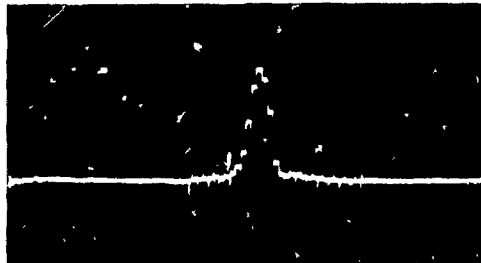
### Laser beam energy distributions

#### Near field

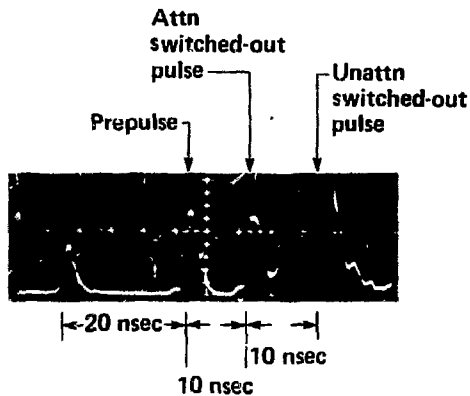


$$\omega_y \approx 1.7 \text{ cm}$$

#### Imaged focal spot



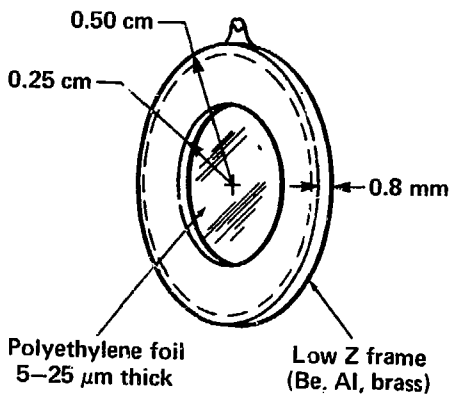
$$\omega_0 \approx 68 \mu\text{m}$$



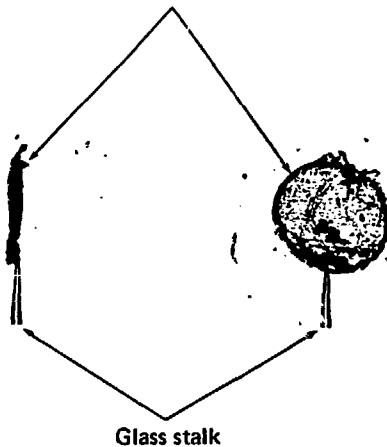
#### Typical prepulse extinction ratios

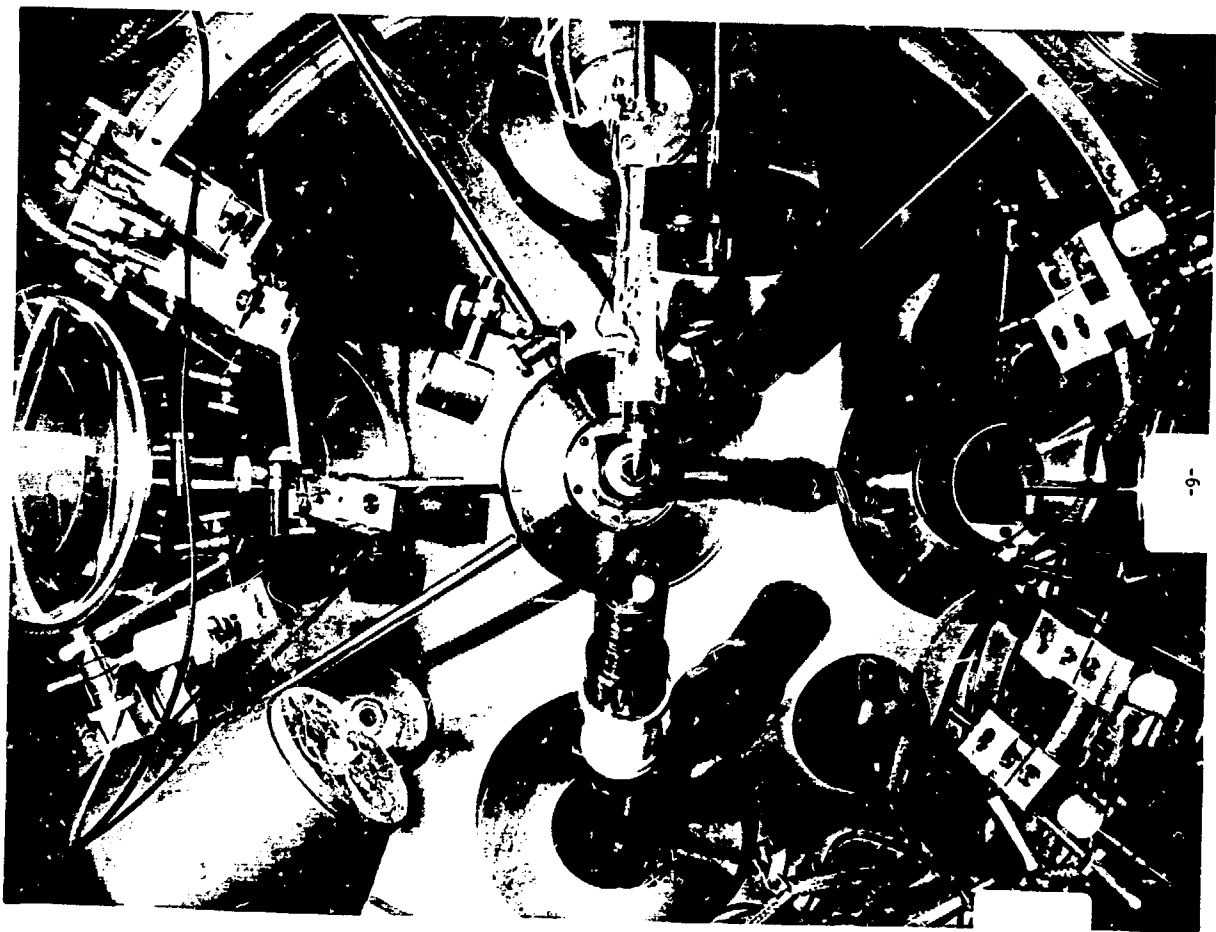
1. At oscillator  $\sim 2 \times 10^6$
2. At target chamber  $\sim 2 \times 10^3$

# TARGETS



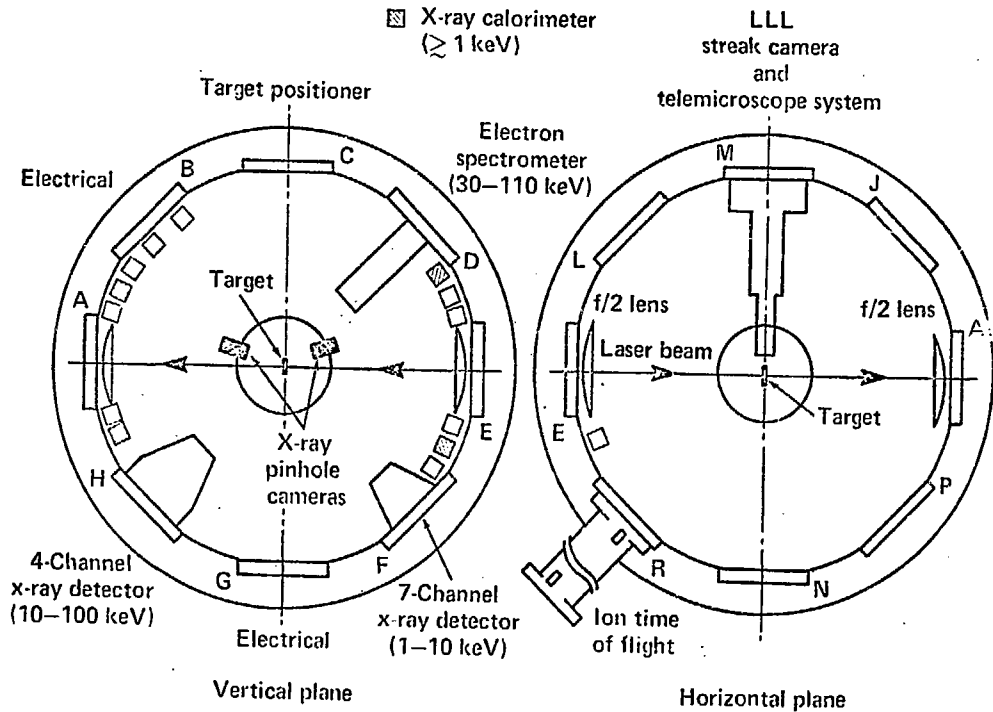
Parylene disk  
~5  $\mu\text{m}$  thick  
~145  $\mu\text{m}$  diameter  
Typical range ~125–200  $\mu\text{m}$  diameter





# PLASMA DIAGNOSTICS CONFIGURATION

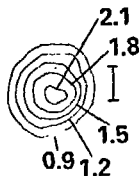
- Ion collector
- ▣ X-ray calorimeter ( $\geq 1$  keV)



**L** SPATIAL DISTRIBUTION OF X-RAY EMISSION

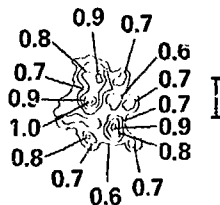
1.06  $\mu\text{m}$  LASER

$I_p \sim 5 \times 10^{13} \text{ W/cm}^2$ ,  
10  $\mu\text{m}$  polyethylene foil

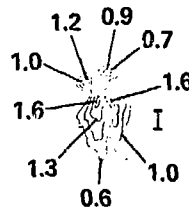


10.6  $\mu\text{m}$  LASER

$I_p \approx 9.4 \times 10^{13} \text{ W/cm}^2$   
5  $\mu\text{m}$  polyethylene foil



$I_p \approx 6.7 \times 10^{13} \text{ W/cm}^2$   
5  $\mu\text{m} \times 170 \mu\text{m}$  dia parylene disk

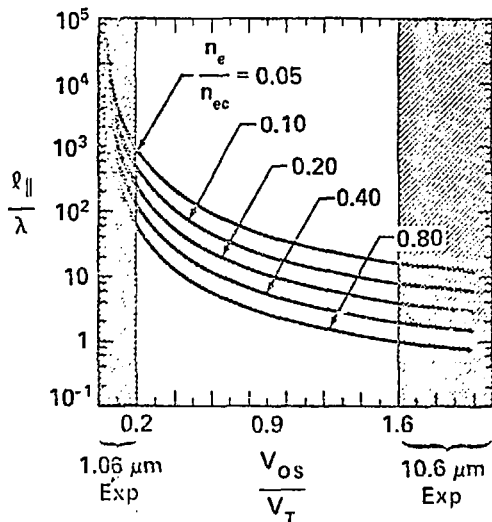


I denotes 100  $\mu\text{m}$

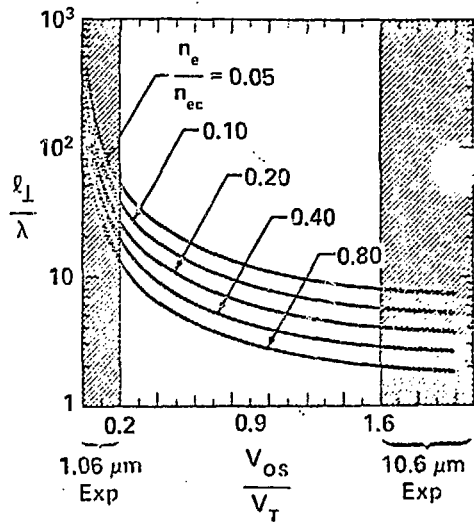
# FILAMENTATION PREDICTIONS (SLAB GEOMETRY)

Ref: Kaw, Schmidt and Wilcox, Phys. of Fluids, 16, 1522 (1973)

Self focus length

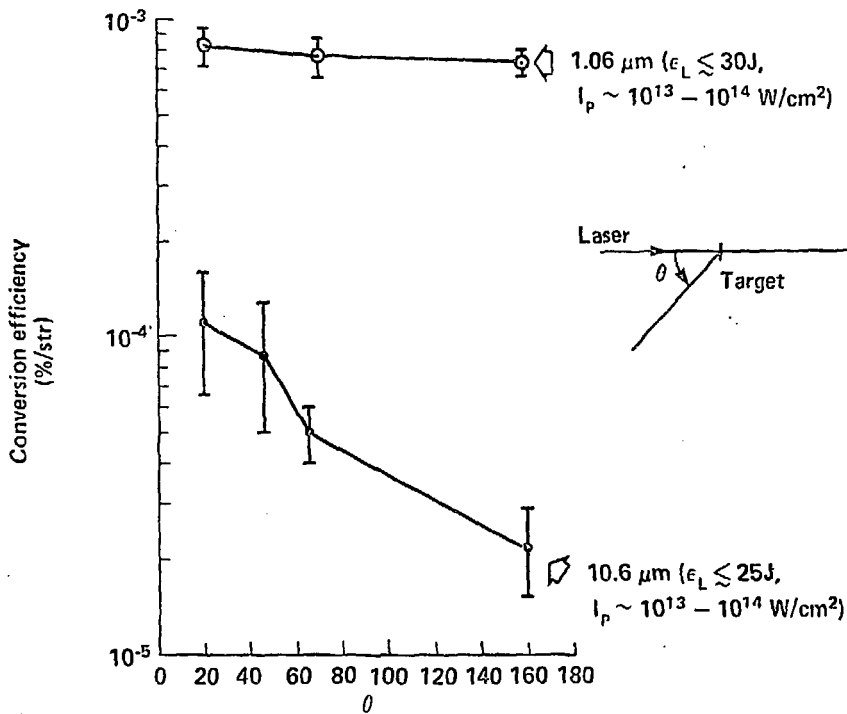


Filament width

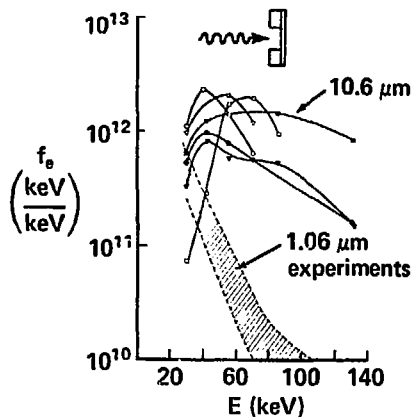


# X-RAY CONVERSION ( $\geq 1$ keV)

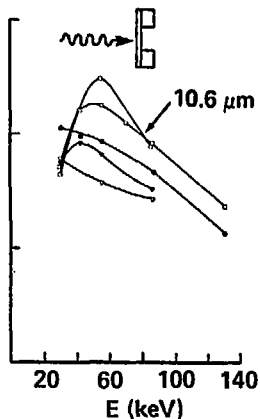
□



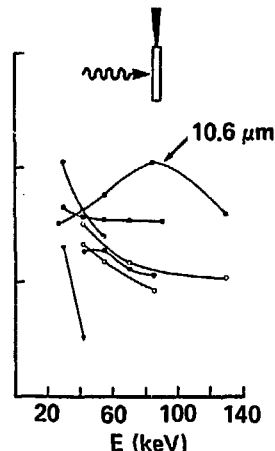
## Target orientation



- $7.1 \times 10^{13} \text{ W/cm}^2$
- ▽  $1.8 \times 10^{14} \text{ W/cm}^2$
- $2.0 \times 10^{14} \text{ W/cm}^2$
- $9.4 \times 10^{13} \text{ W/cm}^2$
- ▼  $8.8 \times 10^{13} \text{ W/cm}^2$
- $7.2 \times 10^{13} \text{ W/cm}^2$



- $2.4 \times 10^{14} \text{ W/cm}^2$
- ▽  $1.8 \times 10^{14} \text{ W/cm}^2$
- $8.5 \times 10^{13} \text{ W/cm}^2$
- $5.8 \times 10^{13} \text{ W/cm}^2$
- ▼  $4.5 \times 10^{13} \text{ W/cm}^2$

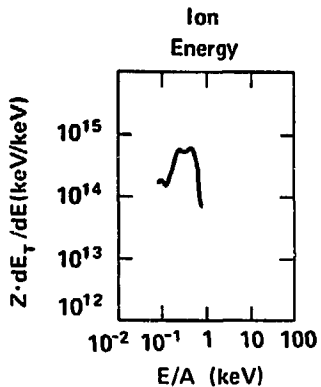


- $5.7 \times 10^{13} \text{ W/cm}^2$
- ▽  $6.7 \times 10^{13} \text{ W/cm}^2$
- $8.4 \times 10^{13} \text{ W/cm}^2$
- $1.1 \times 10^{14} \text{ W/cm}^2$
- ▼  $7.2 \times 10^{13} \text{ W/cm}^2$
- $9.5 \times 10^{13} \text{ W/cm}^2$
- ⊙  $8.9 \times 10^{13} \text{ W/cm}^2$
- ▣  $1.7 \times 10^{14} \text{ W/cm}^2$

# ION EMISSION ENERGY DISTRIBUTIONS

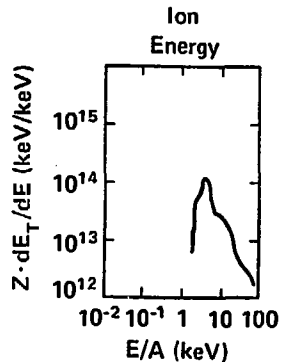
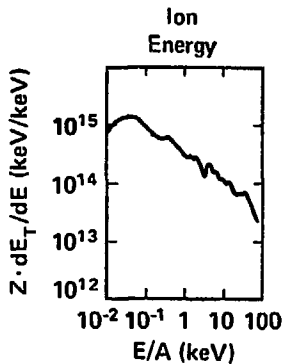
1.06  $\mu\text{m}$  LASER

10  $\mu\text{m}$  polyethylene foil  
 $I_p \cong 5 \times 10^{13} \text{ W/cm}^2$



10.6  $\mu\text{m}$  LASER

5  $\mu\text{m}$  polyethylene foil    5  $\mu\text{m} \times 175 \mu\text{m}$  dia parylene disk  
 $I_p \cong 4.5 \times 10^{13} \text{ W/cm}^2$      $I_p \cong 5.4 \times 10^{13} \text{ W/cm}^2$



# PLASMA EXPANSION AND ACCELERATION

10.6  $\mu\text{m}$  LASER

1.06  $\mu\text{m}$  LASER

10  $\mu\text{m}$  POLYETHYLENE FOIL

$$I_p \approx 5.1 \times 10^{13} \text{ W/cm}^2$$

(BACK SURFACE)



$5 \times 10^6 \text{ CM/SEC}$

$1.4 \times 10^7 \text{ CM/SEC}$

5  $\mu\text{m}$   $\times$  150  $\mu\text{m}$  dia. parylene disk

$$I_p \approx 5.7 \times 10^{13} \text{ W/cm}^2$$



$5.4 \times 10^6 \text{ cm/sec}$

$3.9 \times 10^6 \text{ cm/sec}$

$$I_p \approx 9.5 \times 10^{13} \text{ W/cm}^2$$



$6.4 \times 10^6 \text{ cm/sec}$

$\leq 1.8 \times 10^6 \text{ cm/sec}$